The S-type domain and twin boundaries in plate-like $PbZrO_3$ crystals having complicated twinned structures

1993 J. Phys.: Condens. Matter 5 1419

(http://iopscience.iop.org/0953-8984/5/9/026)

J. Phys.: Condens. Matter 5 (1993) 1419–1426. Printed in the UK

The S-type domain and twin boundaries in plate-like $PbZrO_3$ crystals having complicated twinned structures

L E Balyunis†, V Yu Topolov‡, Ibrahima Sory Bah‡ and A V Turik‡

† Institute of Physics, Rostov State University, Prospekt Stachki 194, Rostov-on-Don 344104, Russia

‡ Department of Physics, Rostov State University, ulica Zorge 5, Rostov-on-Don 344104, Russia

Received 7 February 1992, in final form 14 October 1992

Abstract. Four kinds of S-type domain and twin boundaries in the ferroelectric $R3m$ and antiferroelectric $Pbam$ phases of plate-like $PbZrO_3$ crystals with complicated twinned structures have been described. Conditions for thermal stability of S-boundary orientations in perovskites have been formulated.

1. Introduction

Planar domain or twin boundaries of S type, occasionally found in ferroelectric and related crystals, are characterized by their orientations $n_i(h_i k_i l_i)$ which depend [1] on the unit-cell parameters, polarization direction and other physical properties of the separate domains or twin components. Some perovskites exhibit special cases of such a boundary whose orientation may be a certain function of temperature [2] or vary from sample to sample independent of temperature [3]. The study reported here was intended to provide an optical and crystallographic description of the S-type domain and twin boundaries in the ferroelectric and antiferroelectric phases of lead zirconate ($PbZrO_3$) crystals with complicated twinned structures. It is important to note that these domain (twin) boundaries have not been found in $PbZrO_3$ crystals previously (see, e.g., [4–6]). The results obtained in our work enable classification to be made of the conditions for thermal stability of S-boundary orientations in different perovskite crystals.

2. Experimental results

The investigation was carried out on plate-like $PbZrO_3$ crystals obtained by the flux growth technique from the PbO–B_2O_3–$PbZrO_3$ system. The domain (twin) structure was studied using a MIN-8 polarized microscope with a heating chamber. We did not find any appreciable differences between the domain (twin) patterns on both cooling and heating. In our samples, first-order phase transitions were observed:

$$Pbam_{\text{antiferroelectric}} \underset{481\pm0.5\,\text{K}}{\overset{495.5\pm0.5\,\text{K}}{\rightleftharpoons}} R3m_{\text{ferroelectric}} \underset{490\pm0.5\,\text{K}}{\overset{500\pm0.5\,\text{K}}{\rightleftharpoons}} Pm3m_{\text{paraelectric}}.$$

0953-8984/93/091419+08$07.50

According to the previous papers [5, 7], in the $Pbam$ phase, untwinned plates of as-grown $PbZrO_3$ crystals occur with the two natural orientations distinguished by the extinction position (parallel or symmetric). The major surfaces of the crystal samples with parallel extinction coincide with the orthorhombic (210) plane, while plates with symmetric extinction possess the (001) orientation. The spontaneous antipolarization vector $\pm P_a$ makes an angle of 45° with the plane surface in the former case and lies in the plane of the plate at 45° to its edges in the latter case. In the previous papers the planar 90° and 60° twin boundaries oriented along the {100} and {110} planes, respectively, of the perovskite prototype unit cell [5, 7] as well as two kinds of 90° zigzag boundary and two kinds of 60° zigzag boundary [8] were described. In the $R3m$ phase, $PbZrO_3$ crystals had symmetrical extinction with 71° (109°) domain boundaries oriented along the (100) plane of the perovskite unit cell [5, 9].

We were the first to observe, in the antiferroelectric $Pbam$ phase of plate-like $PbZrO_3$ crystals with complicated twinned structures, the 60° inclined twin boundaries. These boundaries represented a type of S wall (figures 1(*a*) and 1(*b*)) and looked similar to the S-type boundaries in the antiferroelectric $Pba2$ and $P222_1$ phases of $PbHfO_3$ [3]. The 60° boundaries in $PbZrO_3$ crystals with mixed (parallel and symmetrical) extinction were visualized as an array of interference fringes, exactly like the 60° boundaries parallel to the (110) planes of the perovskite unit cell but situated at an angle $\alpha = 6$–$12°$ to the side crystal faces. The angle α, although different in different samples, remained invariable during heating to the transition to the ferroelectric $R3m$ phase. Despite the complicated character of the twinned structure (figure 1(*b*)), possible defects and other inhomogeneities which are responsible for excessive mechanical stresses, the inclined 60° boundaries always retain their planar shape and 45° orientation with respect to the crystal faces or otherwise are describable by the Miller indices (11l).

In $PbZrO_3$ crystals, we were able to distinguish between inclined boundaries either alone or in combination with the usual 60° walls with the (110) orientation, with the 90° walls with the (100) orientation, and with separate 90° wedges (figures 1(*a*) and 1(*b*)). As a special case of matching between the usual 60° components and an array of the 60° and 90° components along the S boundary, one may regard a 60° triplet as consisting of two symmetric-extinction components and a parallel-extinction component. The latter has the form of a thin wedge situated between the former two (in figure 1(*c*), its projection onto a large surface is seen as interference). These triplets occur during the ferroelectric-to-antiferroelectric phase transition owing to the similarity between the 71° (109°) domain structure of the $Pbam$ phase and the 90° twin structure of the $Pbam$ phase [5] and to the deflection of the 71° (109°) domain boundaries from the (100) crystallographic plane in comparison with the 90° twin boundaries (figure 2).

In the ferroelectric $R3m$ phase of $PbZrO_3$, a complicated 71° (109°) domain structure is observed with the boundaries oriented approximately parallel to the {001} planes. Some 71° (109°) domain boundaries may deviate appreciably from a [100]-type direction while remaining normal to the large plate surfaces (as in figure 1(*d*)); hence a more correct notation for such a boundary would be {0k1}, where $|k| \ll 1$. This aspect of 71° (109°) domain boundary orientation suggests that S-type boundaries may be present in the ferroelectric phase. A dependence of the domain boundary orientation on temperature, however, could not be established reliably since the ferroelectric phase exists within a restricted temperature range.

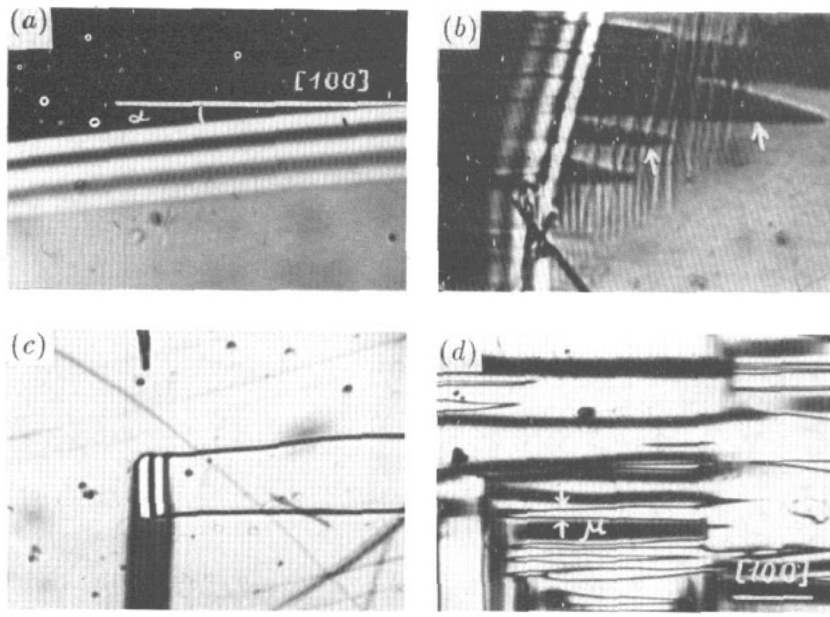

Figure 1. Domain and twin boundaries in (*a*)–(*c*) the antiferroelectric phase (at 290 K) and (*d*) the ferroelectric phase (at 485 ± 5 K) of $PbZrO_3$ crystals: (*a*) separate 60° twin boundary of the S type in the (11*l*) plane; (*b*) an array involving two 60° twin boundaries parallel to the (110) and (11*l*) planes and two 90° walls along (100) and (010) combined with 90° wedges (indicated by the arrow); (*c*) a 60° triplet in a crystal with symmetrical extinction; (*d*) 71° (109°) domain boundaries. (Magnifications, 140×.)

3. Crystallographic interpretation

Crystallographic investigation of the elastic interaction between the twinned regions or between the adjacent twinned phases in $PbZrO_3$ crystals was based on the results in [3, 10]. As pointed out earlier [10, 11], the S-type twin boundaries in the antiferroelectric phase (figures 1(*a*) and 1(*b*)) are related to the presence of both 60° and 90° twin components. These components can match each other along elastically coherent boundaries, or zero net strain planes, if they have equal volume concentrations $t = m$ (figure 3). The orientations $\boldsymbol{n}_1(h_1k_1l_1) \perp \boldsymbol{n}_2(h_2k_2l_2)$ of these planes in the rectangular (X_1, X_2, X_3) system of reference are given by the Miller indices

$$h_1 = k_1 \qquad l_1/h_1 = 4\eta\eta_a(2t-1)/[\eta_a^2 - \eta_b^2 + \eta^2(2t-1)^2] \tag{1}$$

and $h_2 = -k_2$, $l_2 = 0$, in terms of the perovskite unit-cell distortions $\eta_a = (a\cos\omega)/a_c$, $\eta_b = b/a_c$, $\eta = (a\sin\omega)/a_c$, where a, b and a_c are the orthorhombic and cubic unit-cell dimensions, respectively, while ω is the orthorhombic shear angle.

To account for the observed thermal stability of the S-boundary orientation $\boldsymbol{n}_1(T) =$ **constant** in the orthorhombic phases of $PbHfO_3$ [3] and $PbZrO_3$, let us consider the possible reasons for this effect in these and other crystals in some

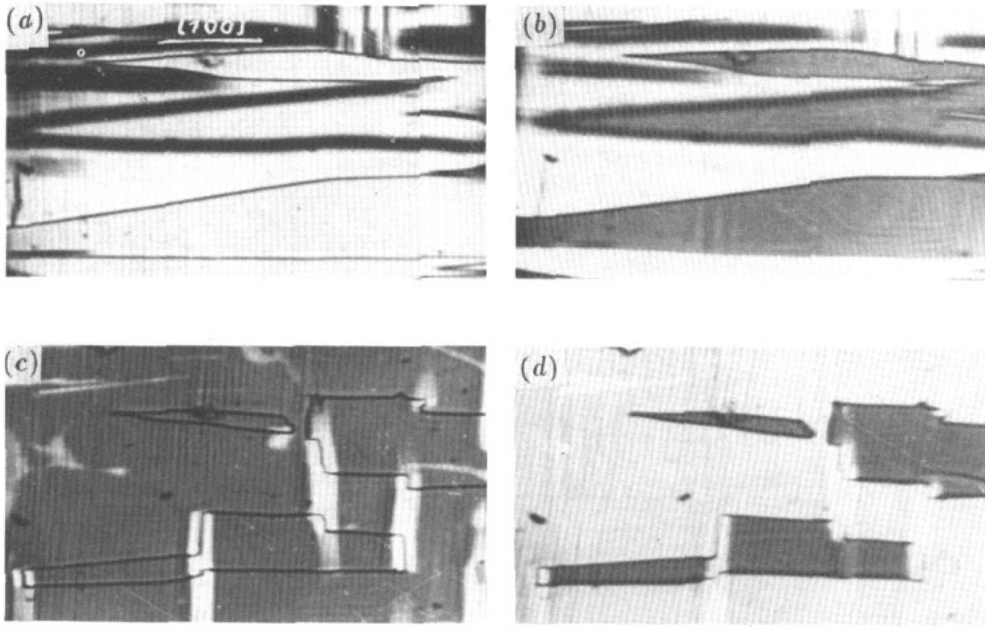

Figure 2. The $R3m \rightarrow Pbam$ phase transition in $PbZrO_3$ crystals with symmetrical extinction ($T = 483 \pm 5$ K): (*a*), (*b*) the crystal in the $R3m$ phase; (*c*), (*d*) the crystal in the $Pbam$ phase. (*a*) and (*c*) were obtained in parallel polarized light; (*b*) and (*d*) were obtained using the mica plate. (Magnifications, 150×.)

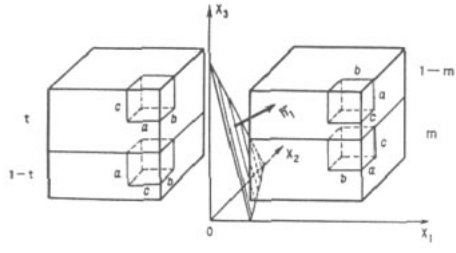

Figure 3. A schematic diagram of the twinned structure containing the S-type boundary (shaded): m, $1-m$, t and $1-t$ are the volume concentrations of the twin components given; n_1 is the normal vector to the boundary.

detail. Here we neglect possible variations in the volume concentrations of the twin components (i.e. $dt/dT \rightarrow 0$) as a result of, for example, a structural phase transition or a large thermal gradient inside a sample. For $n_1(T)$ to be constant, it is sufficient that $d(l_1/h_1)/dT = 0$. On the assumption further that $\eta^2 \ll |\eta_a^2 \pm \eta_b^2|$, which is true for $PbZrO_3$ and other perovskite crystals [12], equations (1) reduce to

$$(\eta_a^2 - \eta_b^2)(\mathrm{d}\eta/\mathrm{d}T) - (\eta/\eta_a)(\eta_a^2 + \eta_b^2)(\mathrm{d}\eta_a/\mathrm{d}T) + 2\eta\eta_a(\mathrm{d}\eta_b/\mathrm{d}T) = 0. \quad (2)$$

In view of the diversity and complexity of the restrictions imposed by equation (2) on the temperature dependences of a, b and ω, we shall confine ourselves to the conditions associated with thermal stability of only one of the unit-cell parameters (table 1 and figure 4). The numerical estimates using unit-cell parameters of $PbZrO_3$ [8] and $PbHfO_3$ [13] indicate that correlation between structural parameters in both cases is regular and obeys the conditions (T1*c*) given in table 1. This is probably because atomic shifts along the b axis and in the a–c plane of the perovskite unit cell are similar in the isostructural orthorhombic phases of $PbZrO_3$ and $PbHfO_3$. In addition, it has been experimentally established [13] that apart from $a(T) = \text{constant}$, $\beta(T) = 90° + \omega = \text{constant}$ is also true for two orthorhombic phases of $PbHfO_3$ (at least within the experimental error in the monoclinic angle β). According to equation (2), this corresponds to the condition $|\mathrm{d}\omega/\mathrm{d}T| \ll 2b\sin\omega\,|(a^2 - b^2)^{-1}(\mathrm{d}b/\mathrm{d}T)|$.

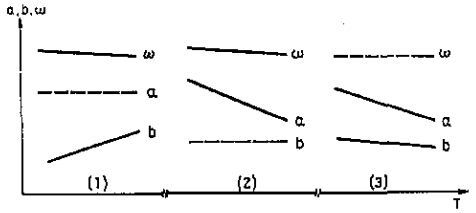

Figure 4. Versions of the temperature dependences $a(T)$, $b(T)$ and $\omega(T)$ corresponding to the conditions (T1), (T2) and (T3) from table 1.

In the course of crystallographic study of the 60° triplets shown in figure 1(*c*), it was found that, whenever $m = 1$, the situation illustrated in figure 3 results. On the basis of the results of the crystallographic description [11], the distortion matrix **M** for the region with the volume concentrations of the twin components t and $1 - t$ and the distortion matrix **N** for the region with $m = 1$ may be written in the form

$$\mathbf{M} = \begin{pmatrix} \eta_b & 0 & 0 \\ 0 & \eta_a & \eta(1-2t) \\ 0 & \eta(1-2t) & \eta_a \end{pmatrix} \qquad \mathbf{N} = \begin{pmatrix} \eta_a & 0 & \eta \\ 0 & \eta_b & 0 \\ \eta & 0 & \eta_a \end{pmatrix}. \quad (3)$$

Conditions for the complete relaxation of the internal stresses at the plane boundary having the normal vector n_1 (figure 3) are determined [11, 14] in terms of the matrix elements M_{ik} and N_{ik}:

$$\det\|D_{ij}\| = 0 \quad (4)$$

and $D_{jk}^2 - D_{jj}D_{kk} \geqslant 0$ $(j, k = 1,2;\ 1,3)$ where $D_{ij} = \Sigma_{k=1}^{3}\,(N_{ik}N_{jk} - M_{ik}M_{jk})$. Then equation (4) is fulfilled strictly only for the matrix elements from equations (3) with the volume concentration $t = 1$, i.e. for elastic matching of two 60° twin components separated by the S wall [1, 11]. In our case, the triplets appear in those crystal regions where certain twin components predominate ($t \ll 1 - t$; $m = 1$ or $m \ll 1 - m$; $t = 1$; see for comparison figures 1(*c*) and 3). This experimental fact corresponds to the approximate fulfilment of equation (4) and to the presence of

Table 1. Conditions on the unit-cell parameters a, b and the shear angle ω used for determination of $n_1(T) =$ constant in the orthorhombic phase of the $PbZrO_3$ crystal. Note that a trivial case where $d\omega/dT \to 0$ simply because $db/dT \to 0$ (T1c) or $da/dT \to 0$ (T2c) is omitted.

Relations between the derivatives		Signs of the derivatives and the relations between the parameters	
$da/dT = 0$	$d\omega/dT = -[(2b\sin\omega)/(a^2 - b^2)](db/dT)$	$\mathrm{sgn}(d\omega/dT) = \begin{cases} -\mathrm{sgn}(db/dT) & \text{for } a > b \\ \mathrm{sgn}(db/dT) & \text{for } a < b \end{cases}$	(T1a) (T1b)
		$d\omega/dT \to 0$ for $b\sin\omega \ll \lvert a^2 - b^2\rvert$	(T1c)
$db/dT = 0$	$d\omega/dT = [(2b^2\sin\omega)/a(a^2 - b^2)](da/dT)$	$\mathrm{sgn}(d\omega/dT) = \begin{cases} \mathrm{sgn}(da/dT) & \text{for } a > b \\ -\mathrm{sgn}(da/dT) & \text{for } a < b \end{cases}$	(T2a) (T2b)
		$d\omega/dT \to 0$ for $(b^2\sin\omega)/a \ll \lvert a^2 - b^2\rvert$	(T2c)
$d\omega/dT = 0$	$da/dT = (a/b)(db/dT)$	$\mathrm{sgn}(da/dT) = \mathrm{sgn}(db/dT)$	(T3)

the mechanical stresses at the twin boundary. The magnitudes of these stresses are not more than $\sigma \simeq c_{ab} D_{ij} \simeq 10^5$–$10^6$ Pa where c_{ab} are elastic moduli of the single crystal (for various perovskite crystals [12], $c_{ab} \simeq 10^{11}$ Pa). Analogous estimates for the stresses arising at the transition between the untwinned $R3m$ and twinned $Pbam$ phases are associated with an unusual behaviour of the unit-cell parameters in $PbZrO_3$ [8]; in the $R3m$ phase $a_R \simeq a$ and $\omega_R \simeq \omega$. Such resulting internal stresses are relatively small and could be removed without the formation of the fourth twin component in the $Pbam$ phase. Owing to the latter circumstance, the triplets observed in $PbZrO_3$ crystals may be considered as compromise or intermediate states between the simplest matching of 60° components [1,11] and a system of 60–90° components (shown in figure 3 and described by equations (1)) along the relaxed S boundary.

In order to describe the elastic matching of twins (71° or 109° domains) in the ferroelectric $R3m$ phase of $PbZrO_3$, we used the scheme shown in figure 3. We specified four domain types (I–IV) described in the (X_1, X_2, X_3) system by the spontaneous polarization vectors $P^{I}(-P_s; P_s; P_s)$, $P^{II}(-P_s; -P_s; -P_s)$, $P^{III}(P_s; -P_s; -P_s)$ and $P^{IV}(-P_s; -P_s; P_s)$ and the volume concentrations m, $1-m$, t and $1-t$, respectively. Analysis of their matching conditions demonstrates that, for any $0 \leqslant m \leqslant 1$ and $0 \leqslant t \leqslant 1$, the boundaries are almost completely relaxed, although they may have a slight curvature as a result of the small excessive stresses. Let us consider two of these matches in more detail.

(i) For $m = t$, one would expect boundaries with $n_1^*(h_1^* k_1^* l_1^*) \perp n_2^*(1/\sqrt{2}, -1/\sqrt{2}, 0)$, where the Miller indices are

$$h_1^* = k_1^* \qquad l_1^*/h_1^* = -[2\eta_a^* + \eta^*(1-2t)]/\eta^* t \simeq -(2\cot\omega_R)/t \quad (5)$$

and the distortions are $\eta_a^* = (a_R \cos\omega_R)/a_c$, $\eta^* = (a_R \sin\omega_R)/a_c$ (a_R and ω_R are the unit-cell parameters in the $R3m$ phase). It follows from equations (5) that $|l_1^*| \gg |h_1^*|$ for small $\omega_R \lesssim 1°$ and any $0 \leqslant t \leqslant 1$ values. The corresponding orientation obtained by the use of a_R- and ω_R-values of $PbZrO_3$ in the $R3m$ phase [8] is described as $(n_1^*, \hat{O}X_3) \lesssim 3'$. So slight boundary deviations from the (001) orientation are probably not detectable by optical and other measurements owing to the real staircase structure of the twin boundaries separating series of the unit cells with $\omega_R \lesssim 6'$.

(ii) Matching of the 109° domain regions (I–II) with a single-domain region (III) represents another interesting example. The respective S-type boundaries are given by the Miller indices $\bar{h}_{1,2} = D_{11}/D_{1,2}$, $\bar{k}_{1,2} = \bar{l}_{1,2} = (D_{12} \pm D'_{12})/D_{1,2}$, where $D_{11} = 8(\eta^*)^2 m(m-1)$, $D_{12} = D_{13} = 2\eta^*(2\eta_a^* + 1)(1-m)$, $D_{22} = D_{33} = D_{11}/2$, $D'^2_{12} = D'^2_{13} = D^2_{12} - D_{11}D_{22}$ and $D_{1,2} = [D^2_{11} + (D_{12} \pm D'_{12})^2 + (D_{13} \pm D'_{13})^2]^{1/2}$. The observed deviations of the boundary orientations by 8–10° from the (001) plane (the angle μ, figure 1(*d*)) may be associated with the presence of the above-mentioned domain (twin) types provided that the condition $m = 1.5$–2% holds. In this case, one of the 109° components has a much greater volume concentration whereas the 180° components have arbitrary volumes.

4. Conclusions

On the basis of optical and crystallographic methods, we have observed and described

the following kinds of the planar S-type boundary which have not been investigated previously in $PbZrO_3$ crystals:

(i) unstrained boundaries between the regions containing 60° and 90° twin components in the $Pbam$ phase;

(ii) domain (twin) boundaries associated with the presence of 109° and 180° twin components and small excessive stresses in the $R3m$ phase.

Moreover, we have studied 60° triple twins (triplets) in the $Pbam$ phase. They can be characterized as intermediate or compromise states between the case of the usual matching 60° twin components and the case of the matching system of 60° and 90° twin components along the S-type boundary.

The analytical conditions determining the thermal stability of the S-boundary orientation $n(hhl)$ have been formulated. These conditions may be applied to different perovskite crystals having complicated twinned structures.

References

[1] Fousek J and Janovec V 1969 *J. Appl. Phys.* **40** 135–42

[2] Ulinzheyev A V, Fesenko E G and Smotrakov V G 1990 *Ferroelectrics* **111** 261–5

[3] Balyunis L E, Topolov V Yu, Turik A V and Fesenko O E 1990 *Ferroelectrics* **111** 291–8

[4] Tanaka M, Saito R and Tsuzuki K 1982 *Japan. J. Appl. Phys.* **21** 291–8

[5] Fesenko O E 1984 *Phase Transitions in Ferroelectric and Antiferroelectric Crystals under Superstrong Electric Fields* (Rostov-on-Don: RGU) p 142 (in Russian)

[6] Roleder K and Dec J 1989 *J. Phys.: Condens. Matter* **1** 1503–10

[7] Iona F, Shirane G and Pepinsky R 1955 *Phys. Rev.* **97** 1584

[8] Balyunis L E, Topolov V Yu, Bah Ibrahima Sory *et al* 1991 *Vsesoyuznii Institut Nauchno-Tekhnicheskoi Informazii* 1665-B91 (in Russian)

[9] Scott B A and Burns G 1972 *J. Am. Ceram. Soc.* **55** 331

[10] Topolov V Yu, Balyunis L E, Turik A V and Fesenko O E 1990 *Ferroelectrics* **110** 41–5

[11] Topolov V Yu 1990 *Proc. All-Union Conf. on Real Structure and Properties of Acentric Crystals (Aleksandrov, 17–22 September 1990)* Part 2 (Blagoveshchensk: USSR Academy of Sciences) p 20 (in Russian)

[12] *Landolt–Börnstein New Series* 1981 *(Zahlenwerte und Funktionen aus Naturwissenschaften und Technik)* Group III, vol 16, ed K-H Hellwege and O Madelung (Berlin: Springer) p 683

[13] Leontiev N G, Kolesova R V, Eryomkin V V *et al* 1984 *Kristallografiya* **29** 395–7

[14] Metrat G 1980 *Ferroelectrics* **26** 801–4